

LETTER TO THE EDITOR

A highly-collimated SiO jet in the HH212 protostellar outflow

C. Codella¹, S. Cabrit², F. Gueth³, R. Cesaroni⁴, F. Bacciotti⁴, B. Lefloch⁵, and M. J. McCaughrean⁶

¹ INAF, Istituto di Radioastronomia, Sezione di Firenze, Largo E. Fermi 5, 50125 Firenze, Italy
e-mail: codella@arcetri.astro.it

² LERMA, UMR 8112 du CNRS, Observatoire de Paris, 61 Av. de l'Observatoire, 75014 Paris, France

³ IRAM, 300 rue de la Piscine, 38406 Saint Martin d'Hères, France

⁴ INAF-Osservatorio Astrofisico di Arcetri, Largo E. Fermi 5, 50125 Firenze, Italy

⁵ Laboratoire d'Astrophysique de l'Observatoire de Grenoble, BP 53, 38041 Grenoble Cedex, France

⁶ University of Exeter, School of Physics, Stocker Road, Exeter EX4 4QL, UK

Received 23 November 2006 / Accepted 12 December 2006

ABSTRACT

Context. In young stars, jets are believed to play a role in removing angular momentum from the circumstellar disk, allowing accretion onto the central star. Recent results suggest that in earlier phases of star formation, SiO might trace the primary jet launched close to the protostar, but further observations are required in order to reveal the properties of this molecular component.

Aims. We wish to exploit the combination of high angular and spectral resolution provided by millimetre interferometry to investigate the collimation and kinematics of molecular protostellar jets, and their angular momentum content.

Methods. We mapped the inner 40'' of the HH212 Class 0 outflow in SiO(2–1), SiO(5–4) and continuum using the Plateau de Bure interferometer in its extended configurations. The unprecedented angular resolution (down to 0''.34) allows accurate comparison with a new, deep H₂ image obtained at the VLT.

Results. The SiO emission is confined to a highly-collimated bipolar jet (width ~0''.35 close to the protostar) along the outflow axis. The jet can be traced down to within 500 AU of the protostar, in a region that is heavily obscured in H₂ images. Where both species are detected, SiO shows the same overall kinematics and structure as H₂, indicating that both molecules are tracing the same material. Transverse cuts reveal no velocity gradient compatible with jet rotation above 1 km s⁻¹, in contrast to previous claims based on H₂ spectra. The central continuum peak is unresolved and close to optically thick, suggesting an edge-on disk with diameter ≤117 AU.

Conclusions. SiO proves to be a powerful tracer of molecular jets in Class 0 sources, in particular of their obscured innermost regions. The very small blue/red overlap in the SiO outflow lobes, despite the nearly edge-on view to HH212, further implies that the high-velocity SiO gas is not tracing a wide-angle wind but is already confined to a flow inside a narrow cone of half-opening angle <6° at ≤500 AU from the protostar. The broad SiO line widths and the transverse velocity gradients both appear significantly affected by internal bowshocks, and should thus be interpreted with caution.

Key words. stars: formation – radio lines: ISM – ISM: jets and outflows – ISM: molecules – ISM: individual objects: HH212

1. Introduction

The launching of jets from young stars is one of the most enigmatic and intriguing phenomena in astrophysics. One fundamental problem to which jets are believed to provide a solution is the removal of angular momentum from the central accreting system, which is required to permit low angular momentum material to fall onto the star. Recent optical observations (e.g. Bacciotti et al. 2002) suggest that atomic jets from evolved T-Tauri stars may indeed transport angular momentum away from the inner regions of the accretion disk. Is the same mechanism at the origin of the molecular jet counterparts observed when the protostar is still deeply embedded in its natal high-density core? To address this question, we have investigated HH212 in Orion ($d = 460$ pc), a highly symmetric bipolar H₂ jet (Zinnecker et al. 1998), associated with a collimated CO outflow (Lee et al. 2006), and driven by a low-luminosity Class 0 protostar, IRAS05413–0104. HH212 provides an optimal situation in which to study jet kinematics, since it lies close to the plane of the sky (4°; Claussen et al. 1998), shows hints of rotation in one H₂ knot (Davis et al. 2000), and is surrounded by a

compact ammonia core rotating about an axis aligned with the jet (Wiseman et al. 2001). As a tracer, we used SiO, which is associated with shocks and generally suffers minimal contamination from infalling envelopes or swept-up cavities (Guilloteau et al. 1992; Hirano et al. 2006).

2. Observations

The SiO observations of HH212 were obtained in January–March 2006 with the IRAM Plateau de Bure Interferometer (PdBI) in France. Two 6-element configurations were used: the new extended A configuration, which includes baselines from 136 m up to 760 m, and the new B configuration, with baselines from 88 m to 452 m. The dual-channel receivers and the correlator were tuned to simultaneously observe the SiO $J = 2-1$ line at 86.847 GHz (resolution: ~0.13 km s⁻¹; bandwidth: ~70 km s⁻¹) and the $J = 5-4$ line at 217.105 GHz (0.11 and 55 km s⁻¹). Continuum emission at both frequencies was also measured. Amplitude and phase were calibrated by observing 0528+134 and 0605–085. The weather conditions were excellent (phase noise rms of 30° at 86 GHz on the 760 m

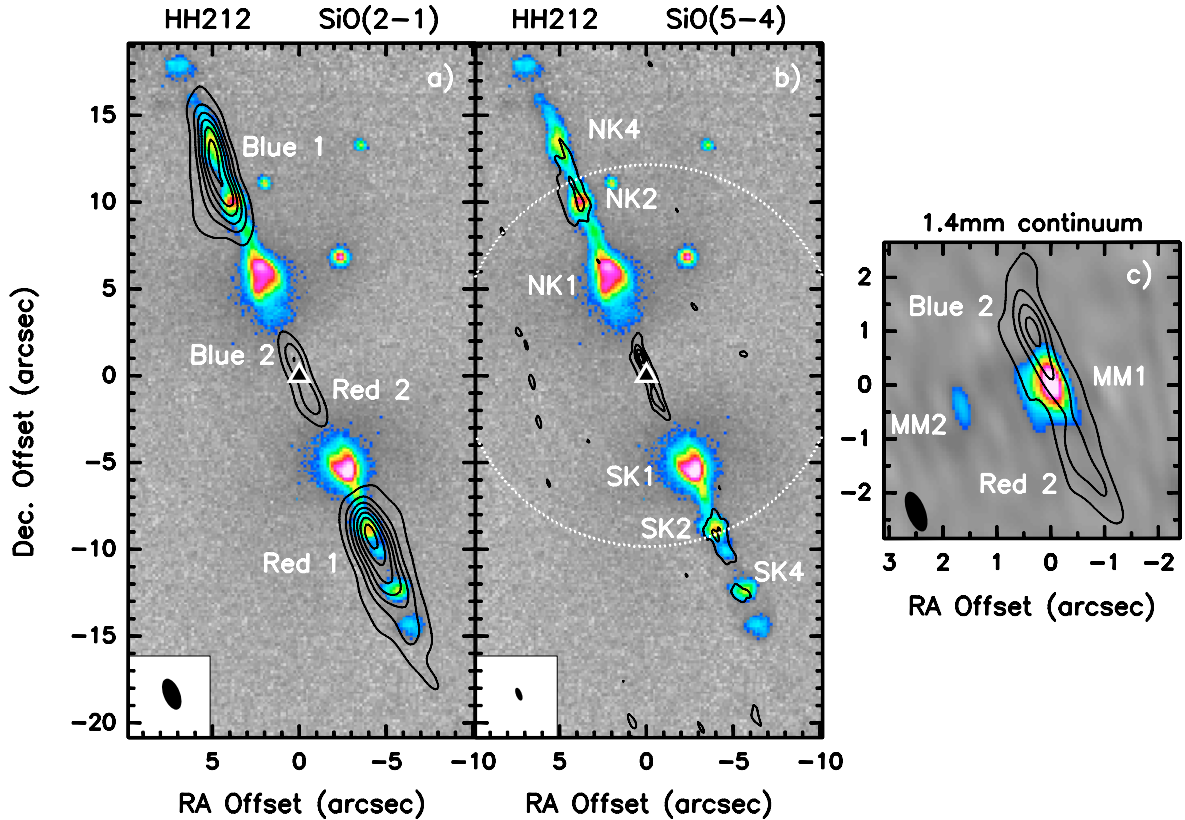


Fig. 1. **a)** Contour map of integrated emission in SiO(2–1) superimposed on the new H₂ image. The SiO emission regions are labelled in white. The filled triangle at (0'', 0'') denotes the driving source MM1 (see Sect. 3.1). Contour levels range from 3 σ (0.22 Jy beam⁻¹ km s⁻¹) to 39 σ by steps of 6 σ . The filled ellipse in the lower left corner shows the synthesised PdBI beam (HPBW): 1''.89 \times 0''.94. **b)** Same as panel **a)** for the SiO(5–4) emission. The dotted circle indicates the primary beam of the PdBI antennae. H₂ knots are labelled in black. Contour levels range from 3 σ (0.42 Jy beam⁻¹ km s⁻¹) to 39 σ by steps of 3 σ . The beam is 0''.78 \times 0''.34. **c)** Inner 5'' of the SiO(5–4) map, superimposed onto the continuum image at 1.4 mm (gray scale and white contours). Continuum contour levels range from 3 σ (1.9 mJy beam⁻¹) to 36 σ by steps of 6 σ . Labels indicate the HH212 driving source (MM1) and a tentative weaker source (MM2). (This figure is available in color in electronic form.)

baselines), leading to a radio seeing of 0''.35. The flux density scale was derived by observing 3C 84 and 3C 279, with an uncertainty of \sim 25%. Images were produced using natural weighting, and restored with clean beams of 1''.89 \times 0''.94 (PA = 22°) at 3.5 mm, and of 0''.78 \times 0''.34 (PA = 21°) at 1.4 mm, using the GILDAS software. The high degree of elongation of the beam is due to the zero declination of the source. However, the spatial resolution is highest perpendicular to the jet direction, making the present observations ideal for the study of the jet collimation and kinematics.

A new, deeper, and higher spatial resolution NIR image of HH212 was obtained using ISAAC on the ESO Very Large Telescope (VLT), Paranal, Chile on November 12, 2005 under good conditions. Although the knots have proper motions of 100–200 km s⁻¹ (McCaughrean et al. 2002), the small epoch difference to the SiO data ensures that the knots have moved only \sim 0''.025, thus facilitating a comparison between the two data sets. A series of images were taken through a 1% wide filter centred on the $v = 1-0$ S(1) line of H₂ at 2.122 μ m. with a total integration time of 32 min per pixel after mosaicing. The image scale was 0''.147 pixel⁻¹, and the spatial resolution is 0''.35 FWHM, similar to our SiO(5–4) map. Accurate astrometry (0''.14 rms) was derived via 21 stars in common with the 2MASS Point Source Catalog. The images have not been continuum-subtracted and thus stellar sources are visible. However, the HH212 jet itself consists almost exclusively of

shocked H₂ line emission and thus there is no confusion along the jet axis.

3. Results and discussion

Emission maps of SiO $J = 2-1$ and $5-4$ are shown in Figs. 1a,b, superimposed onto the nearly contemporaneous H₂ image. The SiO emission is confined to a highly collimated bipolar jet, located along the main outflow axis. The red- and blue-shifted lobes consist of two symmetric pairs of bullets: an outer pair (Blue 1 and Red 1) that follows the H₂ intensity distribution beyond 10'' from the driving source, and a new inner pair within \pm 2'' of the source (Blue 2 and Red 2), with no H₂ counterpart. Figure 1c shows the inner 5'' of the 1.4 mm continuum map, with the SiO(5–4) emission superimposed.

3.1. Continuum sources

The 1.4 mm continuum map (Fig. 1c) shows a bright source (hereafter called MM1) at position $\alpha_{J2000} = 05^{\text{h}}43^{\text{m}}51^{\text{s}}.41$, $\delta_{J2000} = -01^{\circ}02'53''.160$, in excellent agreement with the VLA position at 3.5 cm reported by Galván-Madrid et al. (2004). Comparison with the SiO(5–4) map clearly indicates that MM1 is the driving source of the molecular jet. In addition, we have a tentative detection at $S/N \simeq 6$ (\sim 4 mJy) of a secondary peak (hereafter MM2) at $\Delta\alpha = +1''.6$, $\Delta\delta = -0''.5$, which could trace

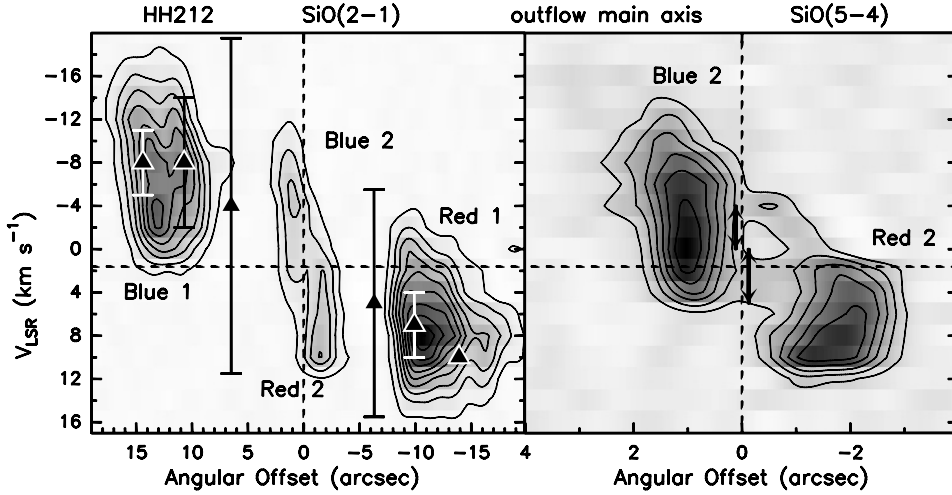


Fig. 2. *Left:* position-velocity cut of SiO $J = 2-1$ along the jet axis (PA = 22°). Contour levels range from 1.4 K to 27.5 K by 2.9 K (8σ). Dashed lines mark the position of MM1 and the cloud V_{LSR} (+1.6 km s⁻¹; Wiseman et al. 2001). Filled triangles with error bars show the velocity centroid and intrinsic FWHM of H₂ knots (Takami et al. 2006). *Right:* zoomed-in PV cut of the inner jet in SiO $J = 5-4$. Contour levels range from 3 K to 21 K by 3 K (4σ). Black arrows show the velocity range of H₂O masers $\pm 0.1''$ from the protostar (Claussen et al. 1998).

an embedded companion. Only MM1 is bright enough to be detected at 3.5 mm, with a flux of 6 mJy. Gaussian fitting in the UV plane at 1.4 mm shows that MM1 is associated with an unresolved peak ($\leq 0''.26$) with a faint extension towards SE. The integrated flux at 1.4 mm is 33 mJy, significantly lower than the 110 mJy reported by Lee et al. (2006) in a $2''.5$ beam, indicating that most of the envelope emission has been resolved out by the PdBI. Contamination by free-free emission from the jet is negligible: if we extrapolate the flux measured by the VLA at 3.5 cm (Galván-Madrid et al. 2004) with a typical $\nu^{0.6}$ slope, the expected contribution is only 0.16 mJy at 3.5 mm. Hence we are dominated by dust continuum. The 1.4 mm flux corresponds to a mean surface brightness of 3.4 K in our beam. Since envelopes and disks are not elongated along the jet axis, the source size is less than $0''.26 \times 0''.26$ and thus the true brightness temperature is quite high: ≥ 13 K. The spectral slope between 1.4 mm and 3.5 mm, derived from UV data, is ~ 2 . Both facts seem to indicate that dust emission is close to optically thick at 1.4 mm. This would suggest that the unresolved mm peak is not tracing the inner parts of the envelope, but a circumstellar disk viewed close to edge-on. The disk diameter would be $\leq 0''.26 = 117$ AU.

3.2. The inner SiO bipolar jet

Our high resolution maps reveal a small-scale pair of SiO emission knots emerging from MM1 and extending out to $1''-2'' = 500-1000$ AU (Fig. 1c). No H₂ counterpart is visible, as the whole structure lies entirely in the high extinction region around the source. The beam-deconvolved transversal size of the two lobes (Blue 2/Red 2) is $\sim 0''.35$, and are thus much more collimated than the hourglass-shaped bipolar cavity seen in ¹³CO on similar scales by Lee et al. (2006). Position-Velocity (PV) diagrams along the jet axis (Fig. 2) further show that the SiO emission extends to high velocities of ± 10 km s⁻¹ from the ambient velocity (+1.6 km s⁻¹; Wiseman et al. 2001), compared to only ± 1.7 km s⁻¹ for ¹³CO (Lee et al. 2006). Hence the SiO lobes include a narrower and faster jet-like component distinct from the swept-up cavity. The maximum radial velocity is similar to the typical centroid velocity of H₂ knots further out (see Fig. 2), arguing that the high-velocity SiO is probably tracing the base of the large-scale (~ 0.5 pc) molecular jet. Correction for

inclination (4° to the plane of the sky; Claussen et al. 1998) gives a full jet speed ~ 140 km s⁻¹, comparable to the proper motion of H₂ knots (McCaughrean et al. 2002). Inner SiO knots were also recently imaged in HH211 down to $\leq 2''$ from the protostar (Hirano et al. 2006; Gueth et al. 2006). Hence SiO appears to be a powerful tracer of the jet base in Class 0 sources.

Hirano et al. (2006) found broad SiO linewidths in the protostar in HH211, which they attributed to a wide angle wind. Such an interpretation is not supported in HH212, however: SiO profiles show little blue/red overlap in each lobe (see Fig. 2), despite the almost edge-on inclination. Assuming a conical wind of constant speed, a half-opening angle $\leq 6^\circ$ is inferred, ruling out a wide-angle wind. The fact that SiO emission stops *precisely* near zero velocity, with an overlap of at most 2 km s⁻¹, would actually suggest that the wind half-opening angle coincides to within 2° with the angle from the plane of the sky¹. Since such a coincidence is statistically unlikely, it appears more probable that high-velocity SiO is confined to *less* than 4° from the jet axis (thus producing no emission at zero velocity) and that SiO emission near systemic velocity is tracing *intrinsically slower*, possibly less collimated material. This slow material may trace unresolved bowshock wings. Indeed, water maser spots observed via VLBI reveal curved bowshocks at $\pm 0''.1$ from the protostar, covering a range of radial velocities (black arrows in the right panel of Fig. 2; Claussen et al. 1998). Given the restrictive excitation and coherence conditions for maser amplification, the observed velocity range is less than the full range in the bow. Hence, internal bowshocks could contribute significantly to the broad SiO line widths. Intrinsic gradients in jet speed (due e.g. to time variability, or to a range of launch radii) may also be present.

3.3. The outer SiO bullets

At distances of $10''$ and beyond, the spatial correspondence between SiO and H₂ is very good. The two symmetric elongated

¹ The wind half-opening angle, θ_{max} , is related to the angle to the plane of the sky, α , by $\tan \theta_{\text{max}} = (R - 1)/(R + 1) \tan \alpha$ where R is the ratio (in algebraic value) of maximum to minimum radial velocities in a given lobe. In HH212, $v_{\text{max}} > 10$ km s⁻¹, $-2 < v_{\text{min}} < 0$ km s⁻¹, and $\alpha = 4^\circ$ yield $R < -5$ and $\theta_{\text{max}} = 4^\circ - 6^\circ$.

SiO bullets (Blue 1/Red 1) peak towards H₂ knots SK2-SK4 and NK2-NK4 (note that the SiO(5–4) image is affected by primary beam attenuation at large distances from the centre ($FWHM = 22''$). SiO emission is also seen between and beyond these knots, with a morphology similar to that in H₂ (Fig. 1). The correspondence between SiO and H₂ in the outer bullets is also excellent in radial velocity, as shown in the PV diagram in Fig. 2 (left panel). The SiO(2–1) profiles peak within 2 km s^{-1} of the H₂ centroid. Hence SiO appears to trace the same jet as H₂, confirming the conclusion of Takami et al. (2006) based on SiO(8–7) profiles at much lower angular resolution ($22''$). The SiO line profiles are broader than towards the inner knots, but they show the same extension down to zero velocity and small degree of red/blue overlap, suggestive of internal bowshocks. Line profile asymmetries between the two lobes indicate slight differences in shock structure despite the highly symmetric knot spacings.

In contrast to the excellent agreement between SiO and H₂ beyond $10''$, we find a striking lack of SiO emission towards the brightest H₂ knots (SK1, NK1). A similar effect was observed towards the HH211 jet, where the brightest, bow-shaped H₂ knots also lack an SiO counterpart (Hirano et al. 2006). One possible explanation would be that SK1 and NK1 trace more powerful shocks where SiO does not form/survive or where the SiO excitation is extremely high and consequently the low-J transitions are very weak. The detection of [Fe II] emission in SK1 and NK1 (Zinnecker et al. 1998; Caratti o Garatti et al. 2006), their clear bow-shock geometry (see Fig. 1), and their 3–4 times broader linewidth compared to other H₂ knots in HH212 (Fig. 2) support this hypothesis. Estimates of SiO excitation and abundances will be presented in a separate forthcoming paper.

3.4. Search for jet rotation

Davis et al. (2000) reported a centroid velocity shift of $+2.3 \text{ km s}^{-1}$ from NW to SE across knot SK1 which they attributed to jet rotation, based on its agreement with the rotation sense of the ammonia protostellar core (Wiseman et al. 2001). Although SK1 is not detected in SiO (see 3.3), we can test this interpretation in the other knots, as rotation speeds should remain roughly constant once the jet has achieved cylindrical collimation (see Pesenti et al. 2004).

Figure 3a presents PV diagrams across the jet in SiO(5–4) for each emitting region. No shift of the intensity peak is seen across Blue 1 on the scales $\pm 0.5''$ investigated by Davis et al. (2000). On the other hand, a clear gradient is observed across the Red 1 bullet (Fig. 3, bottom panel), with a shift of -6 km s^{-1} over $\sim 1''$ from NW to SE. However, the gradient goes in opposite sense to the rotation pattern of the NH₃ core, ruling out that we are observing rotation of a centrifugally-driven MHD jet. The fact that the centroid of Red 1 is slightly displaced from the jet axis, i.e. that outer SiO bullets are slightly misaligned with respect to the inner SiO jet, suggests that this effect is due instead to a kinematical asymmetry in the shocked material, possibly related to the H₂ jet wiggling apparent in Fig. 3b. Since SK1 traces a much wider bowshock than the SK2-SK4 knots in Red 1 (see Fig. 1), its transverse velocity gradient measured in H₂ could easily be affected by similar asymmetries, and should be interpreted with great caution. The innermost SiO knots (Blue 2/Red 2) do not show signs of transverse velocity shifts above 1 km s^{-1} , consistent with the high-velocity SiO jet being practically unresolved transversally. Higher angular resolution would be needed to constrain the level of jet rotation.

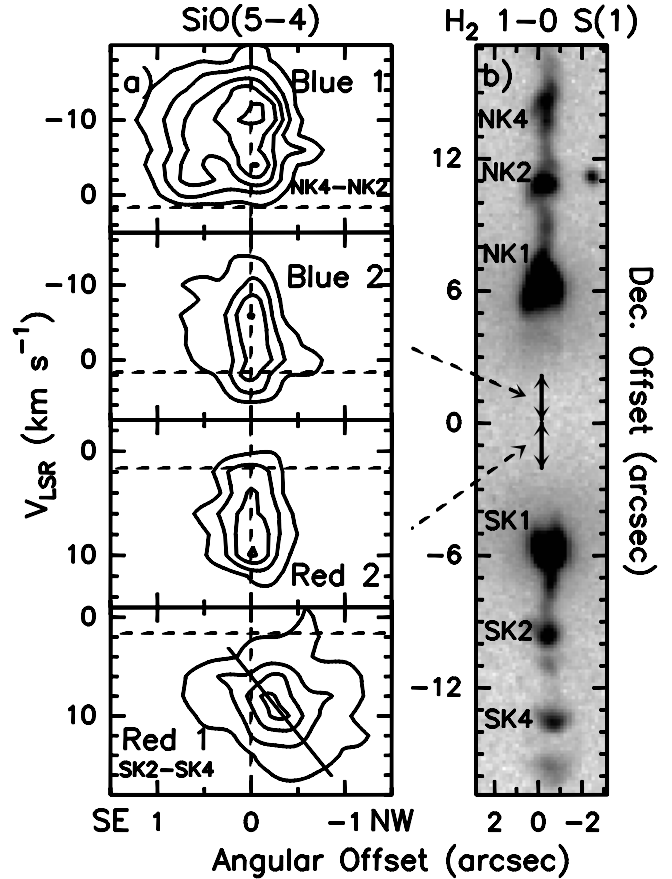


Fig. 3. a) PV cuts in SiO(5–4) perpendicular to the jet axis, averaged over each of the four SiO bullets. Contour levels start at 3σ with steps of 6σ . They range from 1 K to 9.3 K (Blue 1), 2.7 to 14.5 K (Blue 2/Red 2), and 1.7 to 11.6 K (Red 1). Dashed lines mark the jet axis at PA = 22° and the V_{LSR} of the cloud ($+1.6 \text{ km s}^{-1}$; Wiseman et al. 2001). A solid line shows the velocity gradient across Red 1. b) Zoom-in of the H₂ image highlighting the jet wiggling. Vertical black arrows indicate the declination range of the Blue 2/Red 2 inner jet.

Acknowledgements. We wish to thank B. Nisini for helpful discussions and suggestions. This work is supported by the European Community's Marie Curie Research Training Network JETSET under contract MRTN-CT-2004-005592. It has benefited from research funding from the European Community's sixth Framework Programme under RadioNet R113CT 2003 5058187.

References

- Bacciotti, F., Ray, T. P., Mundt, R., Eisloffel, J., & Solf, J. 2002, *ApJ*, 576, 222
 Caratti o Garatti, A., Giannini, T., Nisini, B., & Lorenzetti, D. 2006, *A&A*, 449, 1077
 Claussen, M. J., Marvel, K. B., Wootten, A., & Wilking, B. A. 1998, *ApJ*, 507, L79
 Davis, C. J., Berndsen, A., Smith, M. D., Chrysostomou, A., & Hobson, J. 2000, *MNRAS*, 314, 241
 Galván-Madrid, R., Avila, R., & Rodríguez, L. F. 2004, *RMAA*, 40, 31
 Guilloteau, S., Bachiller, R., Fuente, A., & Lucas, R. 1992, *A&A*, 265, L49
 Gueth, F., et al. 2006, *A&A*, in preparation
 Hirano, N., Liu, S.-Y., Shang, H., et al. 2006, *ApJ*, 636, L141
 Lee, C.-F., Ho, P. T. P., Beuther, H., et al. 2006, *ApJ*, 639, 292
 McCaughrean, M., Zinnecker, H., Andersen, M., Meeus, G., & Lodieu, N. 2002, *Msngr*, 109, 28
 Pesenti, N., Dougados, C., Cabrit, S., et al. 2004, *A&A*, 416, L9
 Takami, M., Takakuwa, S., Momose, M., et al. 2006, *PASJ*, 58, 563
 Wiseman, J., Wootten, A., Zinnecker, H., & McCaughrean, M. 2001, *ApJ*, 550, L87
 Zinnecker, H., McCaughrean, M. J., & Rayner, J. T. 1998, *Nature*, 394, 862